SUPPLEMENTAL METHODS

Metabolic Measurements. Oral glucose tolerance tests (OGTT) were performed on mice fasted for 6 hours. Blood glucose levels were determined at 0, 7 15, 30, 60, 90, and 120 minutes after gavage of glucose (2g/Kg body weight, BW) using a Contour TS glucometer (Bayer). For intraperitoneal glucose tolerance tests (IPGTT), mice were administrated intraperitoneal glucose (1g/Kg BW). Fructose absorption was performed as described (1). Briefly, fructose (2mg/g BW, Sigma-Aldrich) was gavaged to chow-fed mice after 16hours fasting. Blood was collected at timed intervals after gavage and fructose concentration measured. For pyruvate tolerance tests, mice fasted 18hours were injected intraperitoneally with sodium pyruvate (Na-p, 2g/Kg BW), and blood glucose measured. For glucagon challenge, mice fasted 6hours were injected intraperitoneally with glucagon (Sigma, Cat#G2044-1mg, 20μg/Kg BW), and blood glucose measured. Jejunal glucose absorption was also determined using isolated loops (2, 3). Briefly, 10 cm of jejunum was perfused with Krebs-Ringer-bicarbonate solution containing 10mM glucose under anesthesia. Perfusion included a 45 min equilibration period followed by three 15 min periods of collection. Glucose absorption was calculated from the average change in glucose concentration in effluent perfusate versus input. The data are presented as μmol/cm/min. Glycogen content was determined using amyloglucosidase as described (4). Briefly, 50 mg of liver was homogenized in 0.5 mL of 1.5M perchloric acid. After 15 min incubation on ice, homogenates were centrifuged at 4000 rpm for 15 minutes. 75μL of homogenate were spotted on 1.5cm×3.5cm Whatman Grade 3 filters. Filters were washed once in 70% ethanol at 4 ^{o}C for 30 minutes and twice at room temperature for 15 minutes. Filters were rinsed with acetone

for 3 minutes at room temperature. After complete drying, 1.0 mL of amyloglucosidase reaction mixture (containing 0.04% amyloglucosidase in 50 mMNaOAc) was added and incubated at 37^{o}C for 90 minutes. Glucose concentration was measured with Wako Kit (FuJi Film Wako #997-03001). Glycogen content was calculated as mg glucose per 100 mg wet weight liver. Hepatic glycogen was also visualized by PAS staining on slides prepared from formalin fixed tissue. Oxygen *(*O_2) consumption, heat production, respiratory exchange ratio (RER, or respiratory quotient), and carbon dioxide (CO_2) production rates were determined using an Oxymax indirect calorimeter (Columbus Instruments, Columbus, OH) or PhenoMaster (TSE Systems, Inc. Germany) as described(5, 6). Mice (5 mice per genotype) were housed individually in the chamber and allowed to acclimate for several hours before the start of data collection. O_2 and CO_2 levels were sampled every 2 min up to 20 hours, and the data for each 30-min interval were averaged.

For measuring GLP-1 and GIP levels, blood samples were treated with EDTA (1.5 μg/ml blood) and an inhibitor of dipeptidyl peptidase (DPP)-4 (10 μl/ml blood; Linco Research Inc., MO, USA). Blood samples were collected both at 0 and 20 min after glucose gavage. GLP-1 and GIP concentrations were measured with total GLP-1 kit (Meso scale Discovery, MD, USA) and RAT/Mouse GIP (Total) ELISA kit (Millipore, MA, USA) respectively according to manufacturer instructions. GLP-1 ELISA plate was read on MSD 2400 sector imager (Meso scale Discovery, MD, USA). GIP plate was read on a Synergy HT microplate reader Gen5™ system (BioTek). Gastric empting was measured as described (7). Briefly, 15min after a gavage of phenol red (50μg/ml) at dose of 0.5μg/g BW, the residual phenol red in the stomach was measured spectrophotometrically at 570nm.

For serum Fgf15 levels, blood samples were collected at ~6pm, right before the start of dark phase. All the blood samples were collected at the same time (in one hour time frame).Hepatic lipids were extracted and triglyceride, free and total cholesterol, measured enzymatically using Fuji Film Wako Kits: L-type triglyceride M kit (catalog number 465-09791, 461-09891), cholesterol E (catalog number 493-17501), Free Cholesterol E (catalog number 435-35801), respectively (Fuji Film Wako Chemicals).

Specific metabolite detection. BA pool size was determined enzymatically as the total BA content of the entire small intestine, gallbladder, and liver, which were homogenized and extracted in ethanol (8, 9). In addition, fecal BA excretion was determined in stool collected from individually housed mice for 72 h. For each determination, 200 mg triplicate aliquots of dried feces were extracted into ethanol as described. BAs in liver, intestine and intestinal lumen were separately extracted in ethanol. Total BAs were determined enzymatically by Bioquat Kit (Catalog Number BQ092A-EALD), normalized to tissue weight, and presented as μmol/g tissue. BAs in intestinal mucosa were subjected to Folch extraction and BAs in aqueous phase were determined, and normalized to protein content. Bile acid species were also individually determined by LC-MS/MS, including total muricholic acid (MCA), total glycomuricholic acid (GMCA), total tauromuricholic acid (TMCA), cholic acid (CA), glycocholic acid (GCA), taurocholic acid (TCA), ursodeoxycholic acid (UDCA), glycoursodeoxycholic acid (GUDCA), tauroursodeoxycholic acid (TUDCA), lithocholic acid (LCA), glycolithocholic acid (GLCA), taurolithocholic acid (TLCA), chenodeoxycholic acid (CDCA), glycochenodeoxycholic acid (GCDCA), taurochenodeoxycholic acid (TCDCA), deoxycholic acid (DCA), glycodeoxycholic acid (GDCA), taurodeoxycholic acid (TDCA).

Briefly, the liver, intestine and fecal samples were homogenized in water (4 mL water/g liver, 4 mL water/g intestine, and 12 mL water/g feces). A protein precipitation procedure was used to extract bile acids from 0.05 mL of homogenate or 0.05 mL of 10-fold-water-diluted homogenate in the presence of deuterated internal standards (d4-TMCA, d4-CA, d4-GCDCA, d4-GCA, d4-CDCA, d4-DCA, d4-LCA, d4-UDCA, d4-GUDCA, d4-GDCA, d4-GLCA, d4-TUDCA, d4-TLDCA, d4-TCA, d4-TCDCA, d6-TDCA). The extracts were separated by column-switching high-performance liquid chromatography (HPLC) on a SecurityGuard Gemini C18 (4 x 3 mm) and ACE Excel Super C18 column (3μm, 50 x 4.6 mm). Bile acids and their internal standards were detected by an Applied Biosystems Sciex 4000QTRAP tandem mass spectrometer (MS/MS) equipped with an electrospray ion source in the negative ion mode and multiple-reaction monitoring (MRM) detection. The homogenate concentrations were determined by reference to a calibrator standard curve, converted into tissue concentrations based on an assumed density of 1 for 1g wet weight of liver, intestine, and feces, expressed as nmol/g tissue. Serum BAs from 0.05ml serum or 0.05 mL of 10-fold-water-diluted serum were extracted similarly by protein precipitation. Individual BA were determined as above and expressed as nmol/ml serum. Ratio of Fxr antagonist in nmol to agonist BA in nmol is the sum of MCA+TMCA+UDCA+TUDCA divided by the sum of CA+TCA+GCA+CDCA+TCDCA+DCA+TDCA+LCA+TLCA (10). Ratio of 12-α–OH BA in nmol to non-12-α-OH BA in nmol is the sum of CA+TCA+GCA+DCA+TDCA divided by the sum MCA+TMCA+UDCA+TUDCA+LCA+TLCA+CDCA+TCDCA (11). Fecal neutral sterol excretion determination was conducted on mice individually housed in cages with metal racks and feces collected for 72 hours. 10mg vaccum-dried feces were used for fecal sterol extraction (12). Briefly, 10mg feces were homogenized in 100ul water, 200μg 5α-cholestane was added

as internal control and neutral sterols extracted twice into petroleum ether. The neutral sterol extract was dried, re-dissolved in toluene, derivatized by TMS-silylation, and quantitated by gas chromatography (12). Fecal coprostanol, cholestanone and cholesterol were determined by their relative retention times and abundance in relation to authentic internal standards (Sigma) with concentrations normalized to starting weight of feces. Short chain fatty acid (SCFA) determination was undertaken as described with minor modificatons (13) on cecal contents following addition of internal standards for acetic acid (AA), proprionic acid (PA) and butyric acid (BA) followed by acidification, neutralization, and derivatization with aminomethylphenylpyridinium (AMPP) and 1-ethyl-3-(3-dimethylaminopropyl) carbodiimide hydrochloride (EDC). The volatile short fatty acids and their internal standards were converted into nonvolatile AMPP amides, and the extracts separated by column-switching high-performance liquid chromatography (HPLC) on a SecurityGuard C18 (4 x 3 mm) and ACE 3 C18 column (3µm, 150 x 4.6 mm). Fatty acid derivatives and their internal standards were monitored by an Applied Biosystems Sciex 4000QTRAP tandem mass spectrometer (MS/MS) equipped with an electrospray ion source in the positive ion mode and multiple-reaction monitoring (MRM) detection. Analysis of 7a-hydroxy-4-cholesten-3-one (C4) was undertaken on mouse serum using LC-MS/MS on an Applied Biosystems Sciex 4000QTRAP tandem mass spectrometer with deuterated (d7-C4) internal standards (Washington University Metabolomics Core).

Gene expression analyses. RNA was extracted using TRIzol® Reagent (Invitrogen Life Technologies, Carlsbad, CA) and treated with DNase. Reverse-transcription was performed using the ABI high capacity cDNA reverse transcription kit (Catalog Number 4368814), with

1 μg of total RNA and random hexamers, to generate cDNA. qRT-PCR assays were performed in triplicate on a Step One Plus Sequence Detection System using Fast SYBR Green Master Mix (Cat#4385612, Applied Biosystems). Primer pairs were designed by Primer Express software 3.0 (Applied Biosystems). Sequences of primers are available upon request. Relative mRNA abundance is expressed as fold change compared to mRNA levels in Control mice, normalized to Gapdh. Preparation of whole cell extracts, SDS-PAGE and subsequent immunological detection were conducted as previously described (8, 9). For Western blotting analyses, primary antibodies were used at 1:1000 dilution unless indicated below. Primary antibody against phospho-Akt473 (cell signaling technologies, #9271), p-Akt308 (cell signaling technologies, #4056), total-Akt (cell signaling technologies, #9727), phospho-Gsk (cell signaling technologies, #9322), total-Gsk (cell signaling technologies, #9315), Ampk and ACC antibody sampler kit (cell signaling technologies, #9957), Sirt1 (cell signaling technologies, #3931), Fasn (Abcam, #ab3844) and Gapdh (Santa Cruz, # SC-25778) were used. Densitometric imaging of corresponding bands were determined using Kodak image station 440 CF, and normalized to Gapdh. Hepatic nuclear extracts were prepared by nuclear extract kit (Active Motif #40010) following manufacturer instructions, and probed with antibodies against Foxo1 (cell signaling technologies, # 2880), PGC1α (Calbiochem, #ST1202) and LaminA/C (cell signaling technologies, #4777). Protein expreesion in intestinal mucosa was analyzed using antibodies toFgf15 (gift from Dr. Paul Dawson, 1:300), Glut2 (Millipore # 07-1402) ,Glut5 (Thermo Fisher Scientific. # MA1-036X) and Klf15 (abcam, ab2647, 1:500). Because of strong circadian rhythm of Fgf15 and Klf15 expression (14), the liver and intestine samples used for these genes' expression were collected at ~5 pm (in two-hour time frame, right before the start of dart phase). To evaluate Sglt-1 protein

expression, we prepared intestinal brush- border membrane vesicles using a magnesium mannitol method (15). Briefly, whole cell homogenate from scraped jejunal mucosa were centrifuged at 3000g for 15 minutes. The pellet was dissolved in 10 mM Mannitol/HEPES/Tris solution and 500 mM MgCl2 was added to a final concentration of 10 mM. After centrifugation at 3000g for 15 minutes, the supernatant was collected and re-centrifuged at 30,000g for 30 minutes. The final pellet was resuspended in 300 mM mannitol solution (pH 7.4) containing 300mM mannitol, 20mM Tris/HEPES, 0.1mM $MgSO_4$, 0.02% NaN_3. 30µg of protein from each sample was used for Sglt-1 detection (Millipore #07-1417) by Western blot. Alternatively, Sglt-1 expression was examined by immunohistochemistry.

16S rRNA gene sequencing (mouse cecum samples). Cecal contents were collected at sacrifice and stored at -80°C for subsequent DNA isolation and sequencing. Bacterial DNA from 100mg cecal content was extracted by QIAamp DNA stool kit (Qiagen, Cat No. 51504) and the automated QIAcube (Qiagen) as described (16). Briefly, 100 mg of cecal content was suspended in 1.2 mL of stool lysis buffer in a 2 mL screw cap tube containing a mix of 6-8 zirconium beads (2·3 mm, RPI Corporation, Mount Prospect, IL) and 0.1 mL of acid washed glass beads (0.4-0.6 mm, Sigma, MO). This suspension was homogenized by bead beating (FastPrep 24, MP Biomedical, Santa Ana, CA) (6·0 set point, 2 minutes), heated (10 minutes, 95°C), vortexed (5 minutes), and centrifuged (14,000 x g, 1 minute, room temperature). The supernatant was then treated with InhibitEX (Qiagen), vortexed (2 minutes, room temperature), held at room temperature (3 minutes) to remove inhibitors of subsequent enzymatic reactions, and centrifuged (14,000 x g, 3 minutes, room temperature). 350 µL of clear supernatant was then loaded onto the QIACube rotor adaptor for automated DNA

purification by QIAamp DNA stool protocol. DNA was eluted in 200ul. DNA Sequencing was carried out at the Alkek Center for Metagenomics and Microbiome Research in the Department of Molecular Virology and Microbiology at Baylor College of Medicine (Houston, Texas). The V4 variable region of the 16S rRNA gene was amplified with primers 515F-GTGCCAGCMGCCGCGGTAA and 806R- GGACTACHVGGGTWTCTAAT using the primer design previously described (17). A 1:5 dilution of each sample was made, and 2 µl of each diluted sample was amplified with the following cycling conditions: 95°C for 2 minutes; 32 cycles of 95°C for 20 seconds, 50°C for 45 seconds, 72°C for 90 seconds; 72°C for 10 minutes; hold at 10°C. Single-indexed sequencing libraries were pooled (100 ng per sample) prior to nucleotide sequencing on the Illumina MiSeq instrument. Paired-end sequences were generated using the 2x250 MiSeq Reagent Kit V2 (Illumina). Sequence data were delivered to Washington University School of Medicine for analysis and taxonomic classification.

16S rRNA amplicon classification. Sequence analysis was carried out with Mothur using the methods described by Kozich, et al. (18). Chimeric sequences were screened with UCHIME (19). Sequences were assigned into operational taxonomic units (OTUs) using Mothur's opticlust (20) method, with subsequent cluster threshold of 97% similarity. A naïve Bayesian classifier was used with the Ribosomal Database Project training set (v.9) to taxonomically classify sequences (21). Taxonomy was assigned to the lowest taxonomic level at which 80% confidence was met. Sequence data will be deposited into GenBank under BioProject XX. Accession numbers will be supplied prior to publication. Differential representation of specific taxa was evaluated using LEfSe (22). For LEfSe, the alpha value

for the factorial Kruskal-Wallis test among classes was 0.05, as was the alpha value for the pairwise Wilcoxon test between subclasses. The threshold on the logarithmic linear discriminate analysis (LDA) score was 2.0 for discriminative features.

Statistical analysis. For microbiome metadata analysis, alpha diversity (richness and Shannon diversity) and beta diversity (Bray-Curtis dissimilarity) measures were carried out using the R library vegan (Jari Oksanen, F. Guillaume Blanchet, Michael Friendly, Roeland Kindt, Pierre Legendre, Dan McGlinn, Peter R. Minchin, R. B. O'Hara, Gavin L. Simpson, Peter Solymos, M. Henry H. Stevens, Eduard Szoecs and Helene Wagner (2017). vegan: Community Ecology Package. R package version 2.4-3. https://CRAN.R-project.org/package=vegan). Differences in diversity between groups of mice were compared using the Mann-Whitney test. Principle coordinates analysis of Bray-Curtis dissimilarity scores was carried out using the R statistical program (R Core Team (2015). R: A language and environment for statistical computing. R Foundation for Statistical Computing, Vienna, Austria. URL https://www.R-project.org/.). Differential representation of specific taxa was evaluated using LEfSe (22). For LEfSe, the alpha value for the factorial Kruskal-Wallis test among classes was 0.05, as was the alpha value for the pairwise Wilcoxon test between subclasses. The threshold on the logarithmic linear discriminate analysis (LDA) score was 2.0 for discriminative features. Correlation coefficients were calculated based on the relative abundance of indicated bacteria genus in each mouse fecal microbiota and the mouse's biochemistry measurements by GraphPad Prism 7.02. Significant association was set at $P<0.05$.

16S rRNA gene sequencing, classification and analysis (human stool samples). 5 human subjects from two separate families with abetalipoproteinemia were recruited.

Human stools were collected and stored at -80°C for subsequent DNA isolation and sequencing. Bacterial DNA was isolated using QIAamp DNA stool reagents and protocol as above. Bacterial DNA samples from abetalipoproteinemia families were sent to MRDNA (http://www.mrdnalab.com/) for 16S rRNA gene sequencing by MiSeq (Illumina). 16S rRNA gene V4 variable region PCR primers 515/806 with barcode on the forward primer were used, using the HotStarTaq Plus Master Mix Kit (Qiagen, USA) under the following conditions: 94°C for 3 minutes, followed by 30 cycles of 94°C for 30 seconds, 53°C for 40 seconds and 72°C for 1 minute, after which a final elongation step at 72°C for 5 minutes was performed. After amplification, PCR products were checked in 2% agarose gel to determine the success of amplification and the relative intensity of bands. Multiple samples were pooled together (e.g., 100 samples) in equal proportions based on their molecular weight and DNA concentrations. Pooled samples were purified using calibrated Ampure XP beads and the pooled and purified PCR product used to prepare illumina DNA library. Sequence data were processed using MR DNA analysis pipeline, in which sequences were joined, depleted of barcodes and sequences <150bp or with ambiguous base calls removed. Sequences were denoised, OTUs generated and chimeras removed. Operational taxonomic units (OTUs) were defined by clustering at 1% divergence (99% similarity). Final OTUs were taxonomically classified using BLASTn against a curated database derived from RDPII and NCBI (www.ncbi.nlm.nih.gov, http://rdp.cme.msu.edu). Further analysis was done by Mr. DNA using Qiime bioinformatics pipeline. Principle Component analysis was done using unweighted Unifrac distance. The taxonomic summary bar plots were used to visualize abundance at the phylum and genus levels.

Normal human stool samples for *Akkermansia* abundance quantitation: 6 healthy adults were recruited from subjects undergoing outpatient screening colonoscopy. BE-501 is a 29 year old, female, Caucasian; N-1383 is a 55 year old, male, Caucasian; N-1391 is a 70 year old, female, African American; N-1399 is a 46 year old, female, African American, ST-40 is a 36 year old, female, African America; ST-53 is a 35 year old, female, Caucasian. None of the patients were taking lipid lowering medications and none had taken antibiotics in the prior 6 months. Stool samples were collected, stool DNA was isolated and stored as described above until use.

Determination of Total bacterial load and *Akkermansia* abundance. Total bacteria load was quantitated by qPCR described above, using universal primer: forward: AAACTCAAAKGAATTGRCGGGG, reverse: AAGGGTTGCGCTCGTT. 40pg of DNA was used as the template in 15ul qPCR reaction mixture (ABI Fast SYBr Green master mix) and run on StepOne Plus real time PCR system (Applied Biosystems). Copy Numbers were calculated using a standard curve generated with a known structured plasmid DNA and normalized to - gram of cecum content. *Akkermansia* abundance was quantitated by qPCR using the following primer pairs CAGCACGTGAAGGTGGGGAC (Forward), CCTTGCGGTTGGCTTCAGAT (Reverse) (23). The copy numbers were calculated as above and normalized to per nanogram cecal or fecal DNA.

Preparation of cecal slurries or *Akkermansia* for transplant. Cecal contents from 5-7 chow-fed Control or *Mttp-IKO* mice were collected, pooled by genotype, diluted 1:10 in - reduced PBS plus 0.05% L-cysteine-HCL, and filtered through a 100μm cell strainer. The

supernatant slurries were adjusted to 16% glycerol, divided into aliquots (1-2ml), and frozen at -80^{o}C until use. At usage, 200ul-slurry per mouse was gavaged once a day. *Akkermansia muciniphila* strain Muc was obtained from Leibniz Institutes DSMZ-German Collection of Microorganisms and Cell Cultures, DSM No.: 22959 (Braunschweig, Germany) reference PMID: 15388697). *A. muciniphila* was grown at 37 ^{o}C in Brain Heart Infusion Broth supplemented with 0.5% porcine gastric mucin and 0.05% L-cysteine under strictly anaerobic conditions. For use in mouse experiments, *A. muciniphila* cultures were centrifuged in air-tight containers, resuspended in PBS supplemented with 15% glycerol, aliquoted and stored at -80 ^{o}C until use. We confirmed the viability and quantified the amounts of *Akkermansia* by titering on BHI-mucin agar plates right before usage. At usage, 5x10 ^{8} cfu/ 200 µl PBS was gavaged to each mouse once a day.

SUPPLEMENTAL REFERENCES

1. DeBosch BJ, Chi M, Moley KH. Glucose transporter 8 (GLUT8) regulates enterocyte fructose transport and global mammalian fructose utilization. Endocrinology 2012;153:4181-4191.
2. Ogawa E, Hosokawa M, Harada N, Yamane S, Hamasaki A, Toyoda K, Fujimoto S, et al. The effect of gastric inhibitory polypeptide on intestinal glucose absorption and intestinal motility in mice. Biochem Biophys Res Commun 2011;404:115-120.
3. Athman R, Tsocas A, Presset O, Robine S, Roze C, Ferrary E. In vivo absorption of water and electrolytes in mouse intestine. Application to villin -/- mice. Am J Physiol Gastrointest Liver Physiol 2002;282:G634-639.
4. Kir S, Beddow SA, Samuel VT, Miller P, Previs SF, Suino-Powell K, Xu HE, et al. FGF19 as a postprandial, insulin-independent activator of hepatic protein and glycogen synthesis. Science 2011;331:1621-1624.
5. Fernandez-Calleja JMS, Konstanti P, Swarts HJM, Bouwman LMS, Garcia-Campayo V, Billecke N, Oosting A, et al. Non-invasive continuous real-time in vivo analysis of microbial hydrogen production shows adaptation to fermentable carbohydrates in mice. Sci Rep 2018;8:15351.
6. Newberry EP, Xie Y, Kennedy SM, Luo J, Davidson NO. Protection against Western diet-induced obesity and hepatic steatosis in liver fatty acid-binding protein knockout mice. Hepatology 2006;44:1191-1205.
7. Suzuki S, Suzuki H, Horiguchi K, Tsugawa H, Matsuzaki J, Takagi T, Shimojima N, et al. Delayed gastric emptying and disruption of the interstitial cells of Cajal network after gastric ischaemia and reperfusion. Neurogastroenterol Motil 2010;22:585-593, e126.
8. Xie Y, Fung HY, Newberry EP, Kennedy S, Luo J, Crooke RM, Graham MJ, et al. Hepatic Mttp deletion reverses gallstone susceptibility in L-Fabp knockout mice. J Lipid Res 2014;55:540-548.
9. Xie Y, Blanc V, Kerr TA, Kennedy S, Luo J, Newberry EP, Davidson NO. Decreased expression of cholesterol 7alpha-hydroxylase and altered bile acid metabolism in Apobec-1-/- mice lead to increased gallstone susceptibility. J Biol Chem 2009;284:16860-16871.
10. Prawitt J, Caron S, Staels B. Glucose-lowering effects of intestinal bile acid sequestration through enhancement of splanchnic glucose utilization. Trends Endocrinol Metab 2014;25:235-244.
11. Haeusler RA, Pratt-Hyatt M, Welch CL, Klaassen CD, Accili D. Impaired generation of 12-hydroxylated bile acids links hepatic insulin signaling with dyslipidemia. Cell Metab 2012;15:65-74.
12. Xie Y, Kennedy S, Sidhu R, Luo J, Ory DS, Davidson NO. Liver X receptor agonist modulation of cholesterol efflux in mice with intestine-specific deletion of microsomal triglyceride transfer protein. Arterioscler Thromb Vasc Biol 2012;32:1624-1631.
13. Bollinger JG, Naika GS, Sadilek M, Gelb MH. LC/ESI-MS/MS detection of FAs by charge reversal derivatization with more than four orders of magnitude improvement in sensitivity. J Lipid Res 2013;54:3523-3530.

14. Han S, Zhang R, Jain R, Shi H, Zhang L, Zhou G, Sangwung P, et al. Circadian control of bile acid synthesis by a KLF15-Fgf15 axis. Nat Commun 2015;6:7231.
15. Margolskee RF, Dyer J, Kokrashvili Z, Salmon KS, Ilegems E, Daly K, Maillet EL, et al. T1R3 and gustducin in gut sense sugars to regulate expression of Na+-glucose cotransporter 1. Proc Natl Acad Sci U S A 2007;104:15075-15080.
16. La Rosa PS, Warner BB, Zhou Y, Weinstock GM, Sodergren E, Hall-Moore CM, Stevens HJ, et al. Patterned progression of bacterial populations in the premature infant gut. Proc Natl Acad Sci U S A 2014;111:12522-12527.
17. Caporaso JG, Lauber CL, Walters WA, Berg-Lyons D, Lozupone CA, Turnbaugh PJ, Fierer N, et al. Global patterns of 16S rRNA diversity at a depth of millions of sequences per sample. Proc Natl Acad Sci U S A 2011;108 Suppl 1:4516-4522.
18. Kozich JJ, Westcott SL, Baxter NT, Highlander SK, Schloss PD. Development of a dual-index sequencing strategy and curation pipeline for analyzing amplicon sequence data on the MiSeq Illumina sequencing platform. Appl Environ Microbiol 2013;79:5112-5120.
19. Edgar RC, Haas BJ, Clemente JC, Quince C, Knight R. UCHIME improves sensitivity and speed of chimera detection. Bioinformatics 2011;27:2194-2200.
20. Westcott SL, Schloss PD. OptiClust, an Improved Method for Assigning Amplicon-Based Sequence Data to Operational Taxonomic Units. mSphere 2017;2.
21. Wang Q, Garrity GM, Tiedje JM, Cole JR. Naive Bayesian classifier for rapid assignment of rRNA sequences into the new bacterial taxonomy. Appl Environ Microbiol 2007;73:5261-5267.
22. Segata N, Izard J, Waldron L, Gevers D, Miropolsky L, Garrett WS, Huttenhower C. Metagenomic biomarker discovery and explanation. Genome Biol 2011;12:R60.
23. Collado MC, Derrien M, Isolauri E, de Vos WM, Salminen S. Intestinal integrity and Akkermansia muciniphila, a mucin-degrading member of the intestinal microbiota present in infants, adults, and the elderly. Appl Environ Microbiol 2007;73:7767-7770.

Supplemental Figure Legends.

Supplemental Figure S1. Similar energy utilization with reduced gluconeogenesis in *Mttp-IKO* mice compared to controls on chow diet. $Mttp^{f/f}$Villin Cre ER^{T2} mice received either vehicle (Control) or Tamoxifen (*Mttp-IKO*) at ~8 weeks of age. Similar changes in body weight were observed 6 weeks after vehicle or Tamoxifen injection (+2.9±0.2 gram in Controls vs +2.3±0.5 gram in *Mttp-IKO*). (A) to (D) Indirect calorimetry was performed 6 weeks after Tamoxifen or vehicle injection. The data obtained for each 30-minute interval were averaged, and values obtained for that interval for each mouse were averaged, normalized to body weight and plotted versus the time of day. (A) Oxygen consumption (VO2), (B) Carbon dioxide production (VCO2), (C) respiratory exchange ratio (RER), (D) heat generation. No significant differences were found by two-way ANOVA, n=5-6 each group. (E) Reduced gluconeogenesis in *Mttp-IKO* mice was revealed by pyruvate challenge experiment. Mice were fasted for 18hrs, followed by intraperitoneal injection of sodium pyruvate (Na-p). Plasma glucose was monitored and plotted against the indicated time. n=4-5 each. (F) Reduced hepatic mRNA expression of gluconeogenesis related genes in *Mttp-IKO* mice. Livers were harvested after 4 hr fast, and mRNA was extracted, mRNA expression of candidate genes was determined by qPCR. The data are presented as mean ± SEM, *n*=8-9 per group.*p<0.05, unpaired t-test

Supplemental Figure S2. Altered hepatic lipid metabolism on chow with a similar energy utilization on short-term fructose diet in *Mttp-IKO.* (A) Livers were harvested from chow-fed mice after a 4hr fast. Hepatic lipids were extracted and determined enzymatically with normalization to protein content. TG: triglyceride, TC: total cholesterol. FC: Free cholesterol. (B) Hepatic mRNA expression of genes related to lipid metabolism determined by real time quantitative PCR (qPCR), normalized to Gapdh. n=4-8. (C) Protein expression of Sirt1-Ampk-Fas axis was determined by western blot. Left panel: representative images. Right panel: bar graph of densitometric analysis after normalization to GAPDH and controls, n=4-5 each. * p<0.05, **p<0.01, unpaired t-test. (D) to (G) $Mttp^{f/f}$Villin Cre ER^{T2} mice received either vehicle (Control) or tamoxifen (*Mttp-IKO*) at ~8 weeks, then were fed a 60% fructose diet for 10days starting at ~11 weeks. Fructose feeding resulted in a similar weight change in both genotype (+0.7±0.5 gram in Controls vs +0.8±0.2 gram in *Mttp-IKO*). Indirect calorimetry was performed on mice after 10 days fructose feeding. The data obtained for each 30-minute interval were averaged, and values obtained for that interval for each mouse were averaged, normalized to body weight and plotted versus the time of day. (A) Oxygen consumption (VO2), (B) Carbon dioxide production (VCO2), (C) respiratory exchange ratio (RER), (D) heat generation, n=5-6 each group. No significant differences were found by two-way ANOVA.

Supplemental Figure S3. Altered bile acid (BA) profile and reduced ileum Klf15 expression in tissues of chow-fed *Mttp-IKOs*. Bile acid profile was analyzed by LC-MS/MS (Methods). (A) Fecal bile acid profile. The individual bile acid species abundance was normalized to fecal weight. (B) Seral bile acid profile. (C) Ratio of Fxr antagonist to agonist BA in different tissues indicated under the X-Axis. (D) Ratio of 12-α–OH BA to non-12-α-OH B in different tissues indicated under the X-Axis, (defined in Supplemental methods). (E) Increased proportion of conjugated BA (left) and correspondingly decreased proportion of

free BA (right) in *Mttp-IKO* liver, ileum and feces**.** Proportion of conjugated (left) and free BA (right) was calculated as a percentage of total bile acid species determined by LC-MS/MS (Methods). The data are mean ± SEM, n=3-5 per genotype. (F) and (G) Tissue was collected at ~5 pm. (F) Ileum Klf15 protein expression by western blot. Representative image was on top panel and bar graph of densitometric quantitation was on the low panel. (G) Hepatic Klf15 mRNA expression by qPCR. The data are mean ± SEM, n=3-5 per genotype.*p<0.05.

Supplemental Figure S4. **Chow-fed *Mttp-IKO* mice had increased serum incretins (GLP-1 and GIP) with an alteration in tissue Tgr5 mRNA and intestinal Gpr mRNA expression.** (A) Serum GLP-1 level and (B) Serum GIP level are increased in *Mttp-IKO* mice both before and 20min after oral glucose administration. Sera were collected from 3 mice per genotype. (C) *Mttp-IKO* mice exhibit decreased gastric emptying rate. Proportion of gastric phenol red dye remaining in stomach was determined at 15min after oral phenol red gavage (detailed in supplemental method). The data are presented as mean ± SEM, n=3-4 per genotype. *p<0.05, **p<0.01. (D) Selective alteration of Tgr5 mRNA expression in different tissues of *Mttp-IKOs*. mRNA was extracted from jejunum, colon, muscle, epididymal white fat (WAT) and interscapular brown fat (BAT). The relative abundance of Tgr5 mRNA in *Mttp-IKO* mice compared to control was determined by real-time quantitative PCR(qPCR), normalized to Gapdh. The data are presented as mean ± SEM. n=5-6 per genotype.*p<0.05, **p<0.01. (E) Increased Gpr120 mRNA expression in *Mttp-IKO* proximal intestine, while reduced Gpr41 mRNA expression in all the regions of *Mttp-IKO* intestine by qPCR. The data are presented as mean ± SEM. n=5 per genotype.*p<0.05.

Supplemental Figure S5. Alteration in microbe abundance, diversity and phyla profile by fructose diet and host genotypes. (A) Cecal DNA was extracted, total 16S rRNA gene abundance was determined by qPCR with universal primer pairs, normalized to cecal content weight. n=4-5 each, one-way ANOVA and Tukey's multiple comparison post-hoc test. (B) Shannon diversity and (C) richness indices are decreased by fructose feeding, with no differences by genotype on the same diet. The data are mean ± SEM, n=5 per group.*p<0.05, **p<0.01. (D-G) Both diet and genotype produce distinct phylum in the gut bacterial community. LEfSe analysis was performed on bacterial communities from two different experimental groups (n=5 per group) to compare either diet (same genotype) or genotype (same diet) effect. Only phylum with LDA score over 2 are considered as a signature phylum. (D) reveals the genotype effect on chow fed mice. Chow-fed *Mttp-IKO* mice exhibit enrichment in 2 distinct phyla: Bacteroidetes and Deferribacteres. (E) reveals the genotype effect on fructose fed mice. Fructose-fed *Mttp-IKO* mice exhibit enrichment in three phyla: Firmicutes, Bacteroidetes and Actinobacteria. (F) reveals fructose diet effect on control mice. Fructose-fed control mice exhibit enrichment in three phyla: Bacteroidetes, Proteobacteria and Deferribacteries. (G) reveals combined effects of diet and genotype. Firmicutes is enriched in chow-fed control mice, Bacteroidetes in chow-fed Mttp-IKOs and Proteobacteria and Defferribacteria in fructose-fed controls. No distinct phylum is observed in fructose-fed *Mttp-IKOs.* –C: chow. –F: fructose diet.

Supplemental Figure S6. LEfSe analysis reveals signature genera either with combination effect of diet and genotype or separate effect of diet or genotype. (A) reveals a combined effect of both diet and genotype. LEfSe analysis was performed on bacterial communities from four different experimental groups. Only genera with LDA score over 2 are considered as a signature genus. Each experimental group exhibits its own signature taxa, e.g *Bacteroides* is a signature taxa for Fructose-fed *Mttp-IKO* mice (*Mttp-IKO-F*); *Lactobacillus* is for chow-fed *Mttp-IKO* (Mttp-IKO-C) mice; *Mucispirillum* is for Fructose-fed control (control-F) mice; and *Clostridium_IVa* is for chow-fed control (control-C) mice. (B) to (E) LEfSe analysis was performed on bacterial communities from two different experimental groups (n=5 per group) to compare either diet (same genotype) or genotype (same diet) effect. Only genera with LDA score over 2 are considered as a signature genus. (B) reveals the genotype effect on chow fed mice. Mttp-IKO-C mice exhibit enrichment in 7 distinct genus including *Bacteroides* and *Lactobacillus*. (C) reveals the genotype effect on fructose fed mice. *Mttp-IKO-F* mice exhibit enrichment in 2 genera including *Lactobacillus* and *Lachnospiraceae_unclas*. (D) reveals the diet effect on control mice. Control-F mice exhibit enrichment in 4 genera including *Bacteroides*, *Alistipes Mucispirillum and Proteobacteria_unclass.* (E) reveals the diet effect on *Mttp-IKO* mice. *Mttp-IKO-F* mice exhibit enrichment in 6 genera including *Bacteroides* and *Alistipes*. The first letter in front of genus indicates the highest taxonomic resolution. c: class level, o: order level, f: family level, g: genus level._uc: unclassified.

Supplemental Figure S7. Antibiotic treatment reduced gut bacterial load, but did not change the response to fructose feeding in either control *or Mttp-IKO* mice. $Mttp^{f/f}$Villin Cre ER^{T2}mice were treated with antibiotics cocktail (Abx: 0.1% Ampicillin, 0.1% Metronidazole, 0.1% Neomycin, 0.05% Vancomycin in drinking water) for 20 days. From day 6 to day 10, mice were injected with either Tamoxifen or vehicle. From day 11 to day 20, mice were fed 60% fructose diet. (A) Cecal bacterial abundance was dramatically reduced by antibiotic treatment in both genotypes. Cecal content DNA was extracted and bacterial abundance was quantitated by qPCR with universal primer pairs. **p<0.01 compared Abx treatment to non-Abx mice. (B) Antibiotic treatment does not alter hepatic lipid content of either control or *Mttp-IKO* mice. Hepatic lipids were extracted and determined enzymatically. **p<0.01 compared *Mttp-IKO* to control mice. Data are mean ± SEM, n=10-13 per group. (C) Antibiotic treatment does not alter mRNA expression of tested hepatic genes either in control or *Mttp-IKO* mice. (D) Serum 7α-hydroxy-4-cholesten-3-one (C-4) was determined by LC-MS/MS (Supplemental method). Antibiotic treatment does not affect serum C4 concentration in control or *Mttp-IKO* mice, although there is reduced serum C4 in *Mttp-IKO* mice. Data are mean ± SEM, n=4 per group.*p<0.05.

Supplemental Figure S8. Similar total bacterial abundance but reduced diversity associated with enriched *Akkermansia* in MCC mice. (A) Cecal content DNA was extracted, total bacteria abundance was determined by real-time quantitative PCR with the universal primer pair (Methods). (B). Shannon diversity and (C) Richness indices were reduced in MCC. MCC: recipients of *Mttp-IKO* cecal content. CCC: recipients of control cecal content. The data are presented as mean ± SEM, n=5 per genotype. **p<0.01. (D) Enriched *Akkermansia*, *Parabacteoides* and *Clostridium_XIVa* in MCC mice revealed by LEfSe analysis. LEfSe analysis was performed on bacterial communities isolated from MCC and CCC mice

(n=5 per group). Only genera with LDA score over 2 are considered as signature genera. The first letter in front of genus indicates the highest taxonomic resolution. c: class level, o: order level, f: family level, g: genus level. _uc: unclassified.

Supplemental Figure S9. Positive correlations between cecal *Akkermansia* abundance and fecal sterol excretion in murine recipients. (A) Increased *Akkermansia* abundance was observed in MCC mice. Cecal DNA was extracted from recipients as indicated below X-axis. MCC: recipients of *Mttp-IKO* cecal content. CCC: recipients of control cecal content. *Akkermansia* abundance was determined by qPCR and normalized to cecal DNA. n=5 each, **p<0.01, unpaired t-test. (B) to (G) Pearson-Spearman correlation analysis was used to identify the association between *Akkermansia* abundance and recipients' fecal sterol content and/or hepatic lipid content. (B) to (E) *Akkermansia* abundance was positively correlated with FNS (B), fecal cholesterol content (C), fecal cholestanone (D) and fecal coprostanol content (E). (F) and (G) *Akkermansia* abundance was negatively associated with hepatic TG (F) and hepatic TC (G). TG: triglyceride, TC: total cholesterol. n=20 animals, Correlation coefficient (r) is indicated in each graph, p<0.05.

Supplemental Figure S10. *Akkermansia* transplantation did not enrich cecal *Akkermansia* abundance or protect WT mice from fructose induced hepatic steatosis After treatment with an antibiotic cocktail, WT recipient mice were cohoused by group, with each group receiving either PBS or *Akkermansia* ($5x10^8$/cfu), and fed 60% fructose diet for 10 days (Methods). PBS: Phosphate buffered saline transplant recipient. AKK: *Akkermansia* recipient. (A) Hepatic lipids were extracted and assayed as described. (B) Fecal neutral sterol content (right) was determined by GC and normalized to fecal weight. (C) Cecal DNA was extracted from recipients as indicated below X-axis. *Akkermansia* abundance was determined by qPCR and normalized to cecal DNA. The data are presented as mean ± SEM, n= 5 per group. *P<0.05, unpaired t-test.

Supplemental Figure S11. Analysis of bacterial communities by 16S rRNA gene sequencing of stool DNA. Stool DNA from 5 subjects from two Abetalipoproteinemia families were submitted for 16S rRNA sequencing and analysis (Method). (A) Reduced Firmicutes, increased Bacteroidetes in ABL probands compared with their heterozygous parents. Relative abundance of each detectable phylum was present as a proportion of the whole community. Each bar is from one subject indicated below x_axis. k_: kingdom, p_: Phylum. (B) Reduced *Blautia*, increased *Bacteroides* and *Akkermanisa* in ABL patients compared with their own parents. Relative abundance of each detectable genera was present as a proportion of the whole community. Each bar is from one subject indicated below x-axis. The numbers above bar graph are the relative abundance of *Akkermansia* (AKK) in different subjects. X-axis k_: kingdom, p_: Phylum, c_: class, c_: order, f_: family and g_: genus. _uc: unclassified. ABL: abetalipoproteinemia patient. Het: Heterozygous parents of abetalipoproteinemia, proband. ABL 1 is family 1, ABL2 is family 2. Horizontal red bars indicate *Blautia and Bacteroides.*

Supplemental Figure S12. Overview summary of metabolic adaptations following impaired chylomicron assembly with intestinal *Mttp* deletion. Jejunal enterocytes accumulate bile acids (BA) and express increased Fgf15 which, along with ileocyte Fgf15, is

secreted into the portal vein. Luminal BA composition is altered with decreased fecal BA excretion and increased pool size. The net effect of these alterations in enterohepatic BA metabolism (reflecting both Fgf15 and FXR effects) is decreased hepatic BA synthesis, as well as decreased gluconeogenesis and increased hepatic insulin sensitivity. Increased hepatic LXR signaling promotes biliary cholesterol efflux which, in combination with increased enterocyte cholesterol efflux, leads to increased fecal cholesterol and neutral sterol (FNS) excretion. Other metabolic adaptations include increased GIP and GLP1 secretion (likely from intestinal L cells), which may contribute to reduced gastric emptying. Brown adipose tissue also exhibits increased TGR5 expression and may participate in systemic signaling through altered serum BA distribution. Finally, the convergence of changes in luminal BA and FNS are associated with shifts in microbial taxa, including increased abundance of *Akkermansia*, which together contribute to the metabolic adaptations observed. Abbreviations: Chol: cholesterol. Sens: sensitivity. Secr: secretion. Synth: Synthesis.

Supplemental Table S1: Summary of genera demonstrating significant associations with changes in either hepatic lipid content (cholesterol and triglyceride) and/or fecal neutral sterol excretion both in chow and fructose fed mice.

	Hepatic		Fecal Neutral sterol	
	TG	TC/FC	Total	Chol. Dev
Firmicutes_unclas-unk (F)	↑			
Dorea (F)	↓	↓		
Olsenella (A)		↓		
Ureaplasma (T)		↓		
Pseudoflavonifractor (F)			↓	↑
Lachnospiracea_incertae_sedis (F)		↓		
Rikenella (B)		↓		
Streptococcus (F)		↑		
Enterorhabdus (A)		↓		
Alphaproteobacteria_unclas-unk (P)		↑		↓
Bifidobacterium (A)		↓		
Anaerotruncus (F)	↑	↑		↓
Desulfovibrionaceae-unk (P)		↓		
Coriobacteriaceae-unk (A)		↓	↑	↑
Clostridium_XVIII (F)		↑		
Clostridium_XI (F)			↓	↓
Enterobacteriaceae-unk (P)				↑
Deltaproteobacteria_unclas-unk (D)	↓	↓	↑	↑
Staphylococcus (F)			↑	↑
Enterococcus (F)				↑
Bacteroidales_unclas-unk (F)		↓		
Parasutterella (P)		↓		
Desulfovibrio (P)		↑		
Clostridium_XlVa (F)	↓		↑	↑
Barnesiella (B)		↑		
Clostridiales_unclas-unk (F)				↑
Lactobacillus (F)	↓	↓	↑	↑
Parabacteroides (B)				↑
Clostridium_IV (F)			↓	
Helicobacter (P)		↓		
Alistipes (B)		↑		↓
Bacteroidetes_unclas-unk (B)		↓	↑	
Prevotellaceae-unk (B)			↑	
Ruminococcaceae-unk (F)				↑
Mucispirillum (D)		↑		
Porphyromonadaceae-unk (B)		↓		
Akkermansia (V)	↑	↑		↓
Proteobacteria_unclas-unk (P)		↑		
Lachnospiraceae-unk (F)		↓		
Bacteroides (B)		↑		

Red arrow: inverse correlation, green arrow: positive correlation. unclas: unclassified. unk: unknown.
B: Bacteroidetes, F: Firmicutes, P: Proteobacteria, D: Deferribactes. A: Actinobacteria, T: TM7,
V: Verrucomicrobia

Supplemental Table S2: Summary of genera demonstrating significant associations with changes in either hepatic lipid content (cholesterol and triglyceride) and/or fecal neutral sterol excretion in Fructose-fed and CMT-treated mice.

	Hepatic		Fecal neutral sterol	
	TG	TC/FC	Total	Chol. Dev
Proteus (P)		↑		
Anaerostipes (F)		↓		↑
Firmicutes_unclas-unk (F)			↓	↓
Bacilli_unclas-unk (F)		↓		
Blautia (F)		↓		
Enterorhabdus (A)		↑	↓	↓
Erysipelotrichaceae_incertae_sedis (F)		↓	↑	↑
Johnsonella (F)		↑	↓	↓
Desulfovibrionaceae-unk (P)			↓	↓
Betaproteobacteria_unclas-unk (P)			↑	
Coriobacteriaceae-unk (A)	↑		↓	↓
Butyricicoccus (F)		↑	↓	↓
Enterobacteriaceae-unk (B)		↓		
Deltaproteobacteria_unclas-unk (P)		↑	↓	↓
Staphylococcus (F)		↑		
Odoribacter (B)			↓	↓
Enterococcus (F)		↓	↑	↑
Parasutterella (P)	↑			
Erysipelotrichaceae-unk (F)	↑	↑	↓	↓
Desulfovibrio (P)			↓	↓
Clostridium_XlVa (F)		↓	↑	↑
Clostridiales_unclas-unk (F)		↑	↓	↓
Parabacteroides (B)			↑	↑
Bacteria_unclas-unk		↑	↓	↓
Clostridium_IV (F)			↓	
Oscillibacter (F)		↑	↓	↓
Alistipes (B)			↓	↓
Bacteroidetes_unclasd-unk (B)			↓	
Prevotellaceae-unk (B)			↓	
Ruminococcaceae-unk (F)		↑	↓	↓
Mucispirillum (D)		↑	↓	↓
Porphyromonadaceae-unk (B)			↓	
Akkermansia (V)		↓	↑	↑
Lachnospiraceae-unk (F)		↑	↓	↓
Bacteroides (B)			↓	↓

Red arrow: inverse correlation, green arrow: positive correlation. unclas: unclassified. unk: unknown.
B: Bacteroidetes, F: Firmicutes, P: Proteobacteria, D: Deferribactes. A: Actinobacteria,
V: Verrucomicrobia

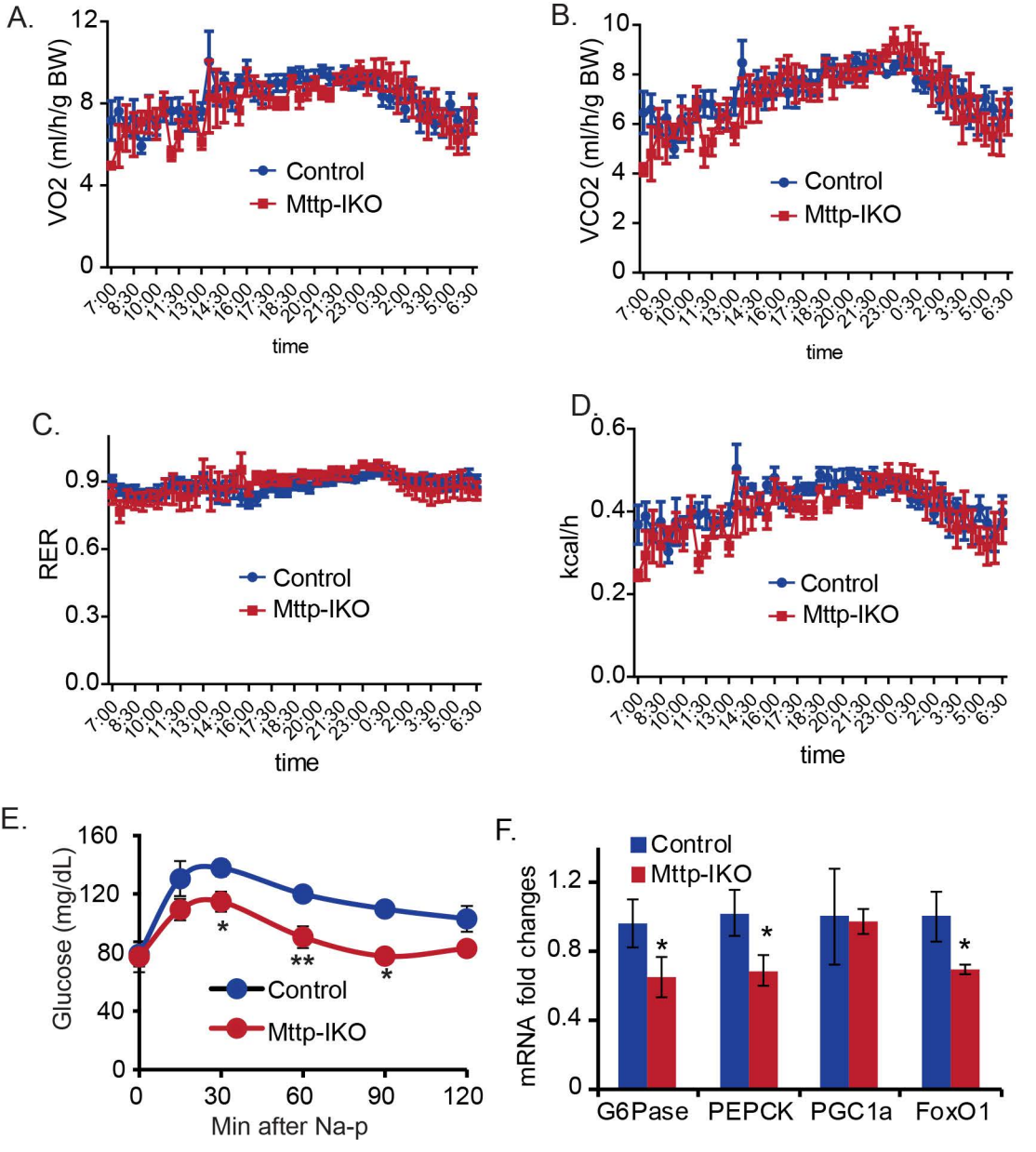

Supplemental Figure S1

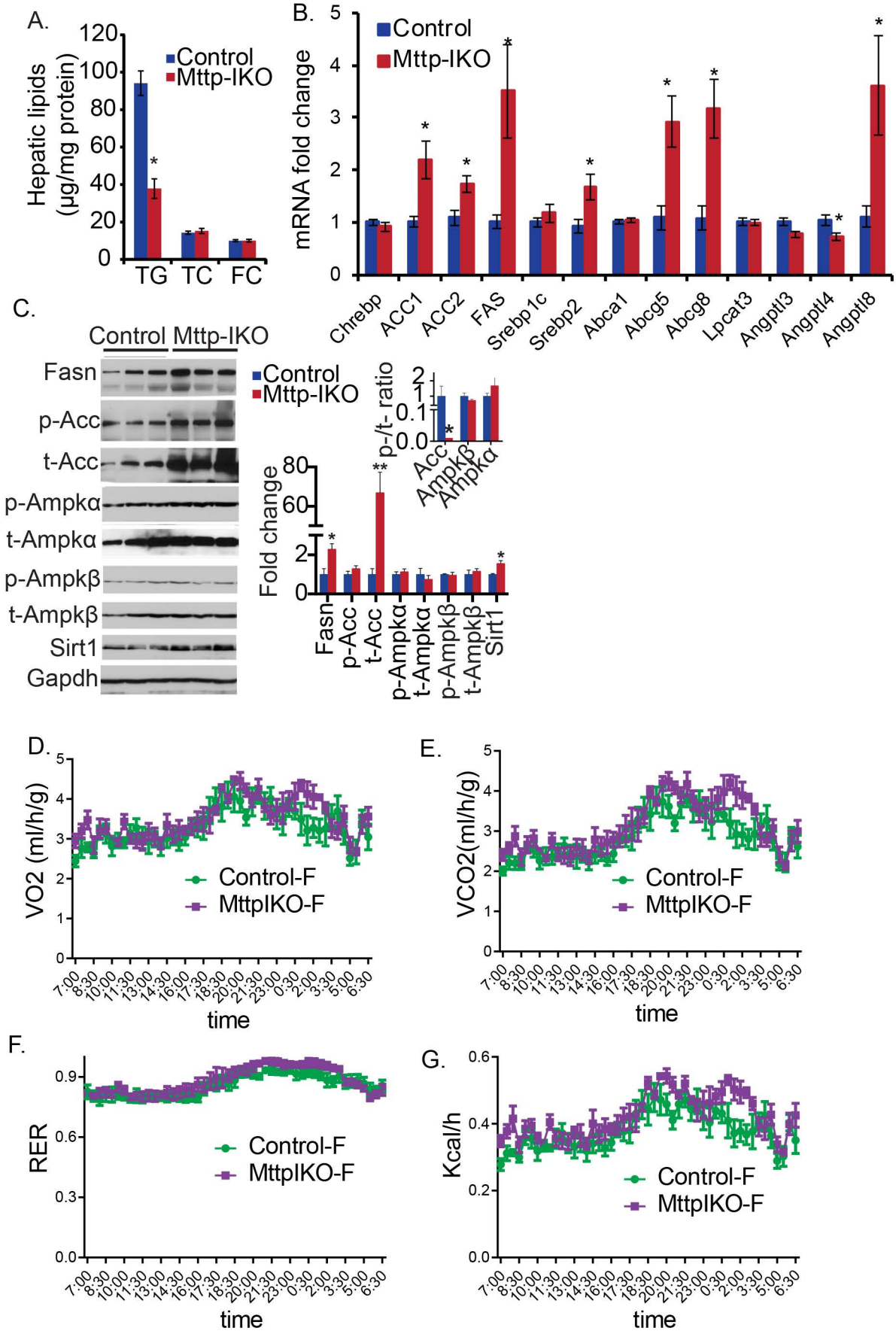

Supplemental Figure S2

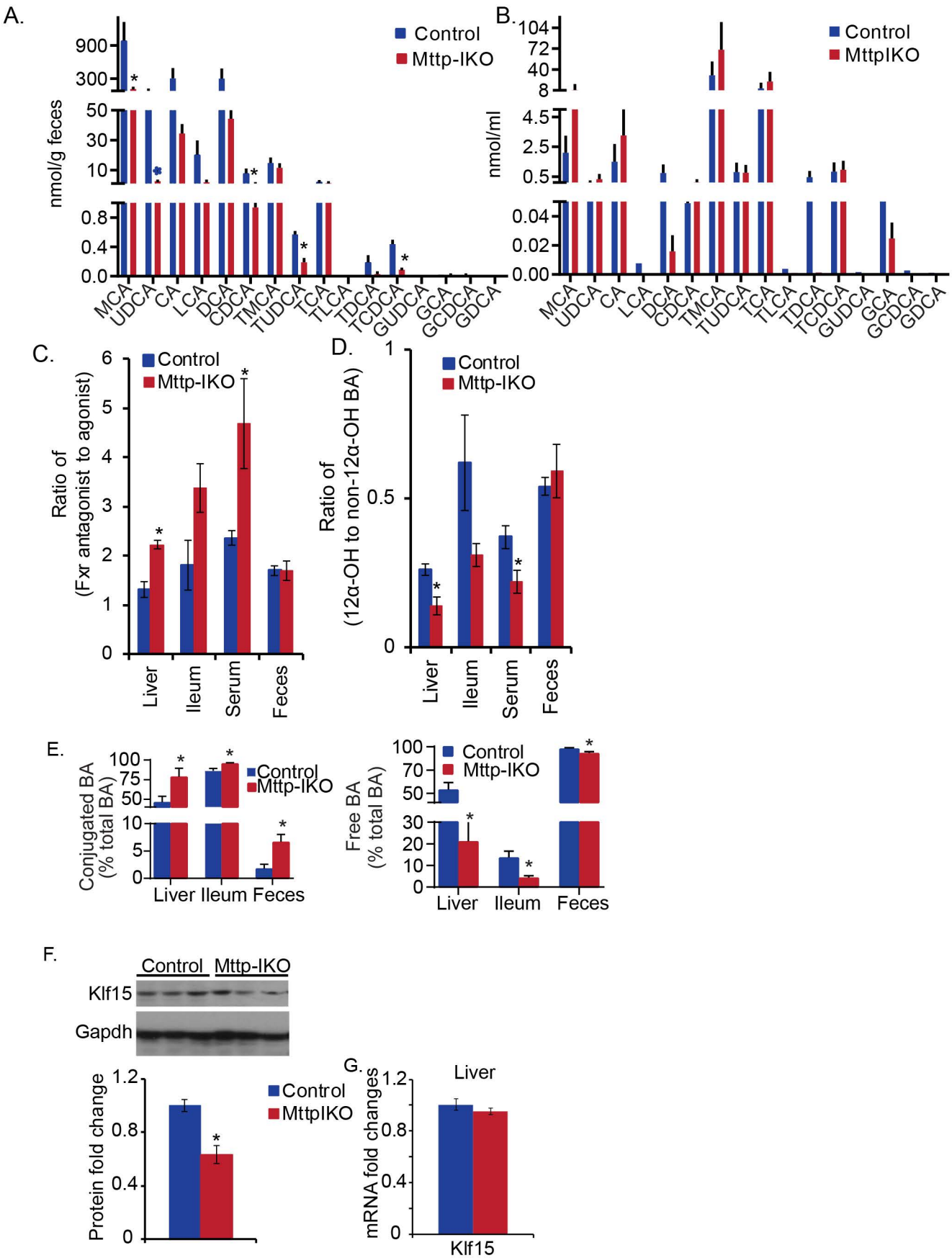

Supplemental Figure S3

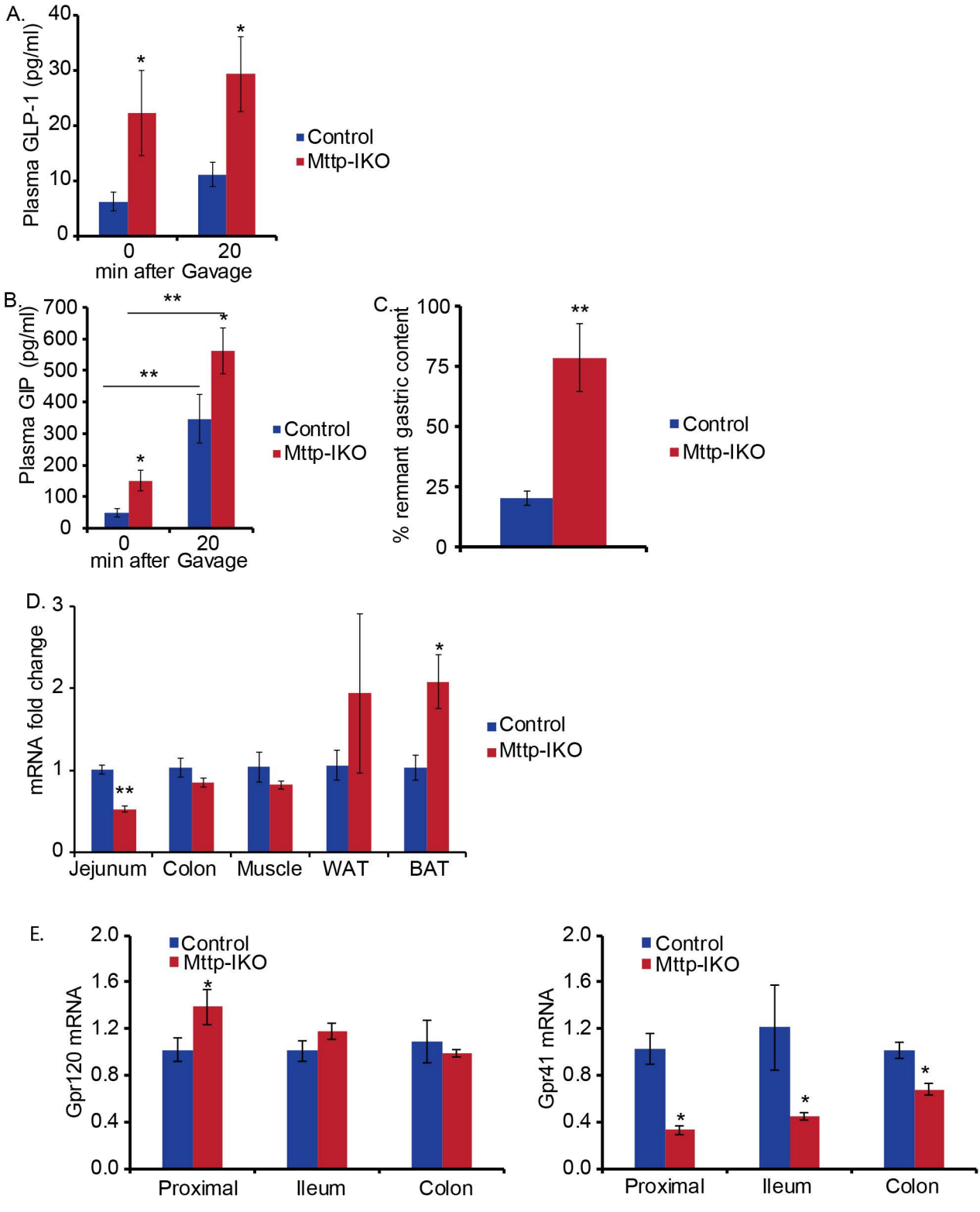

Supplemental Figure S4

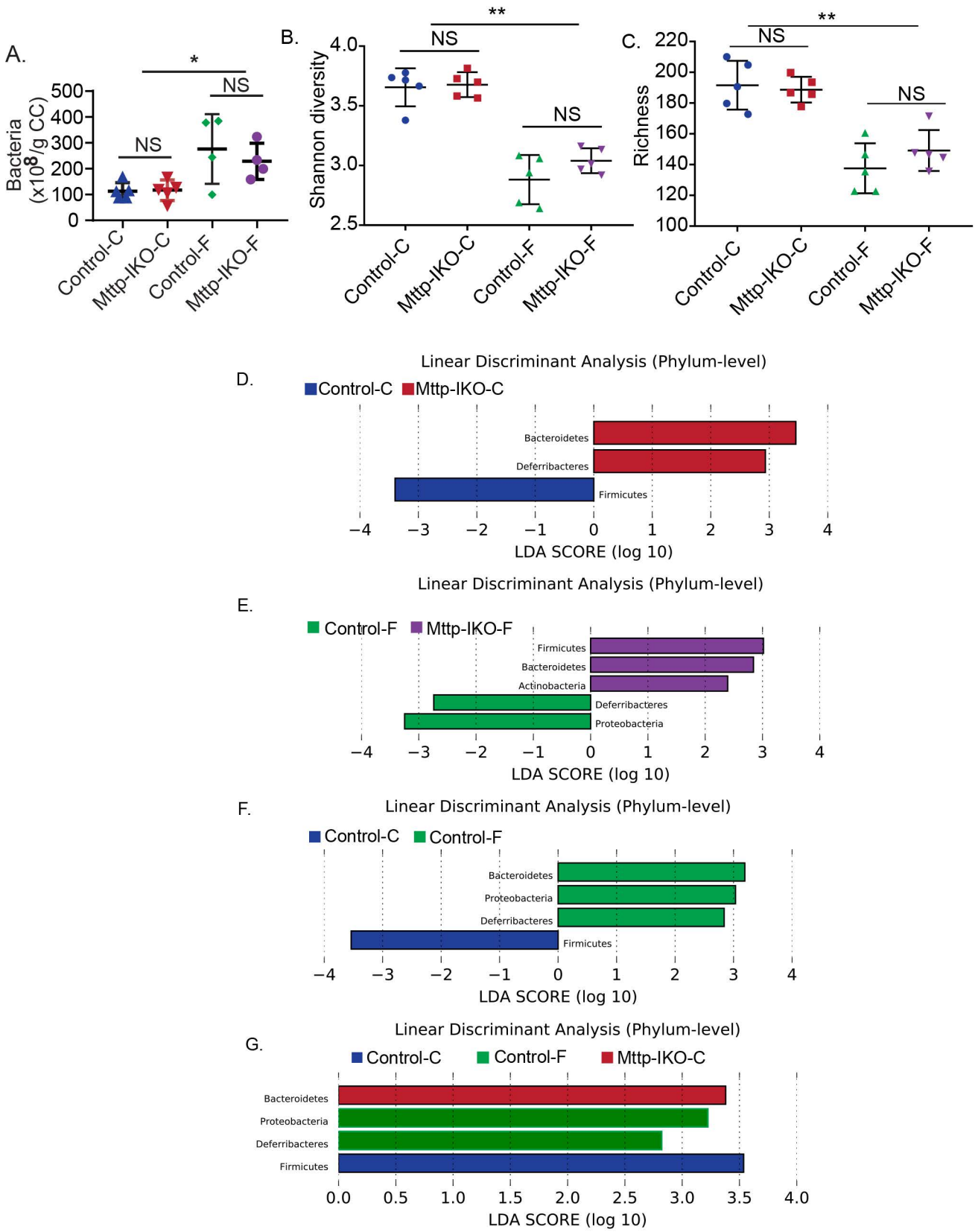

Supplemental Figure S5

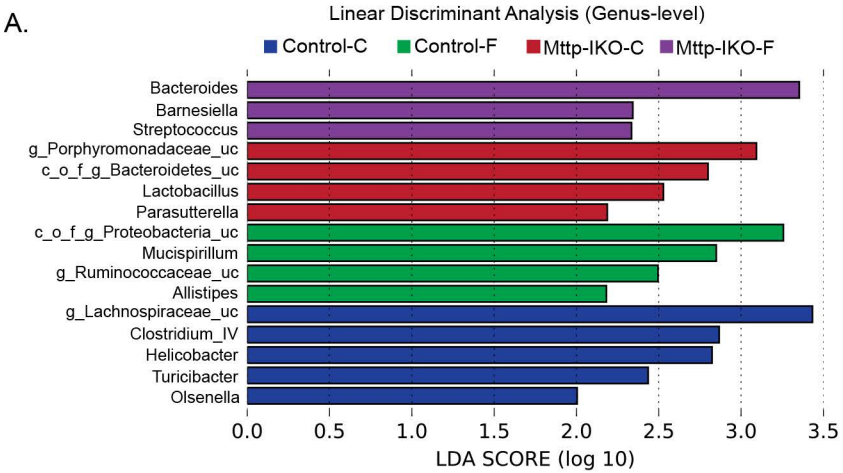

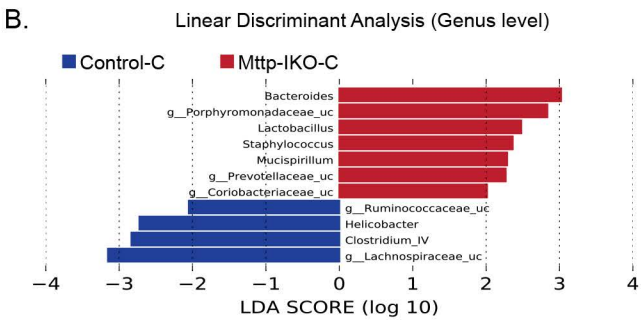

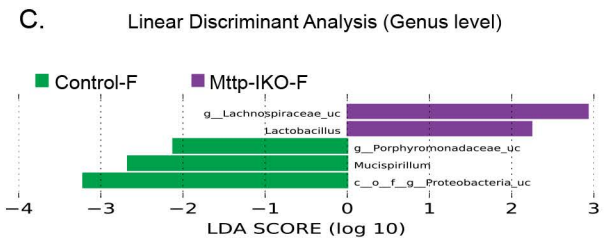

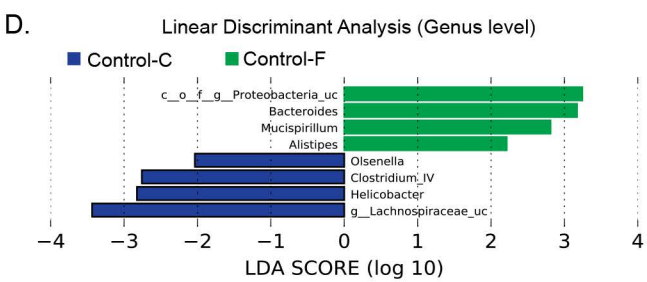

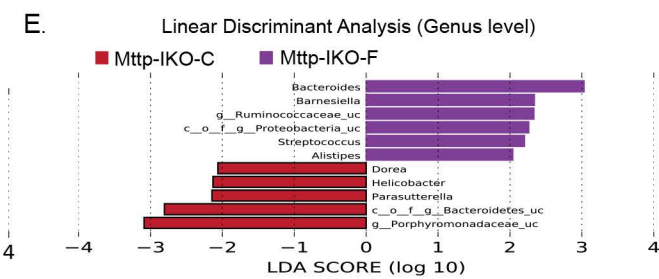

Supplemental Figure S6

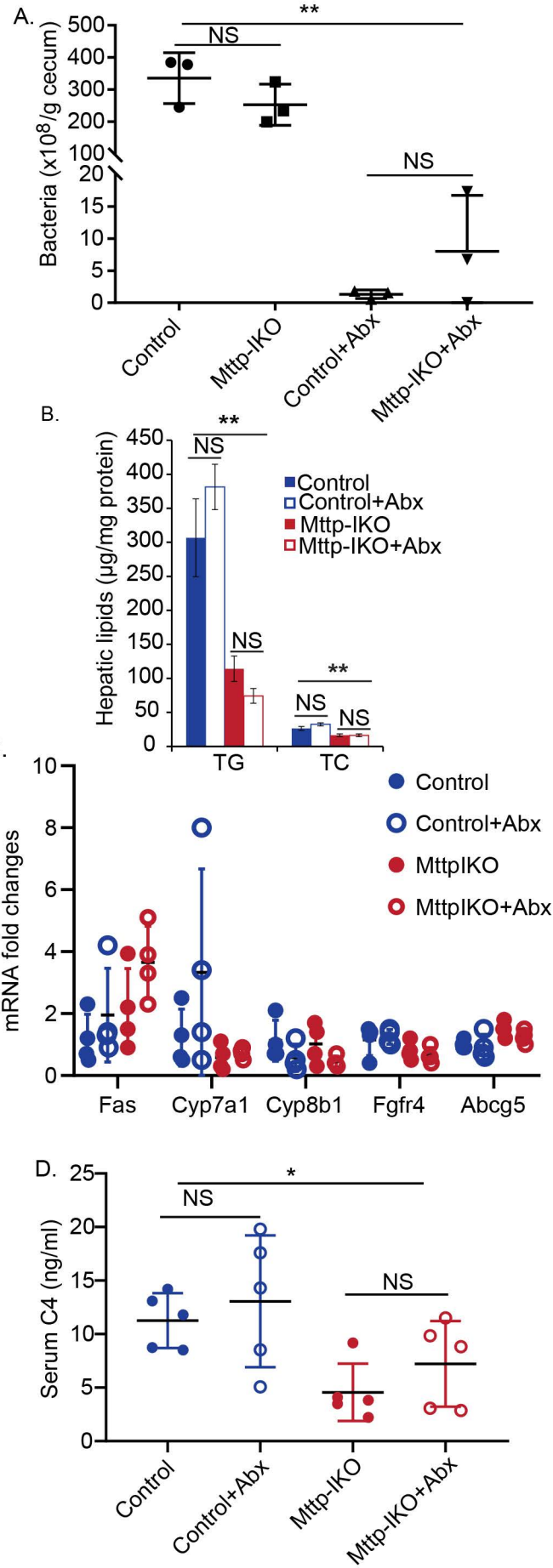

Supplemental Figure S7

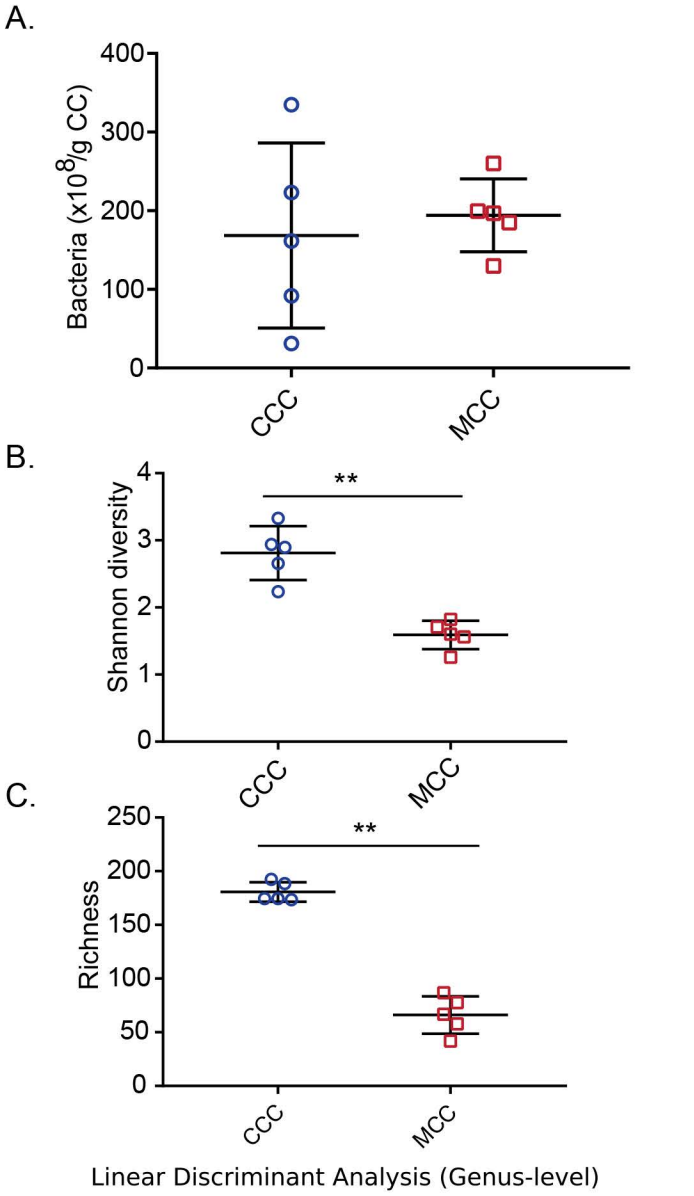

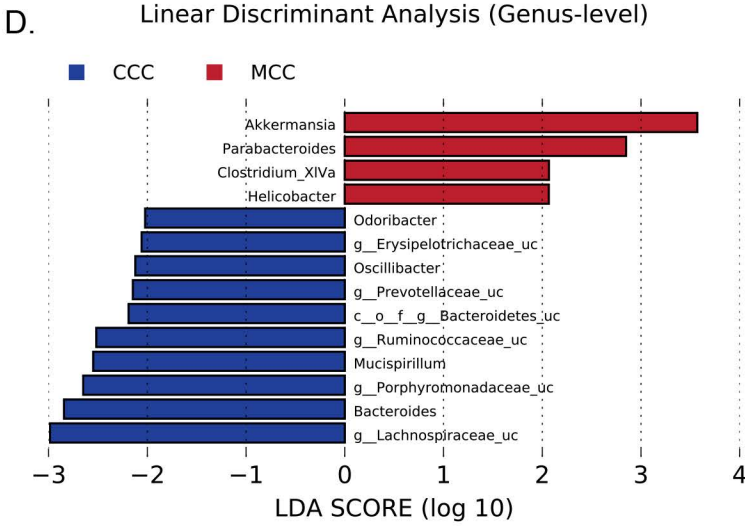

Supplemental Figure S8

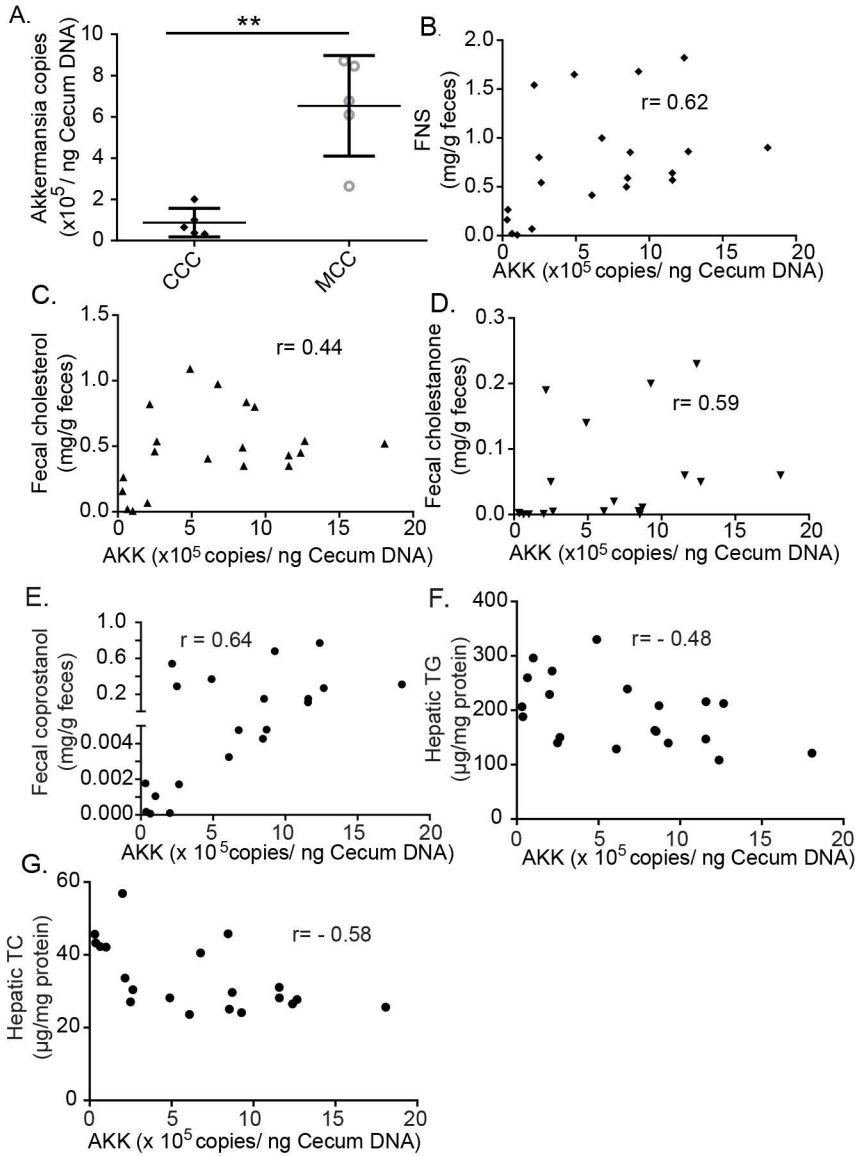

Supplemental Figure S9

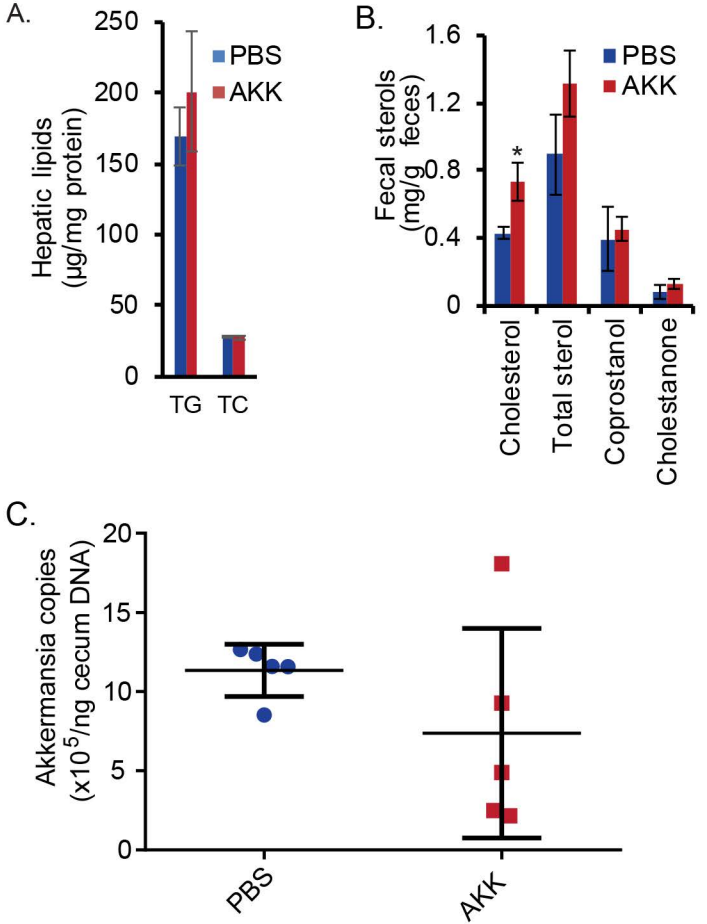

Supplemental Figure S10

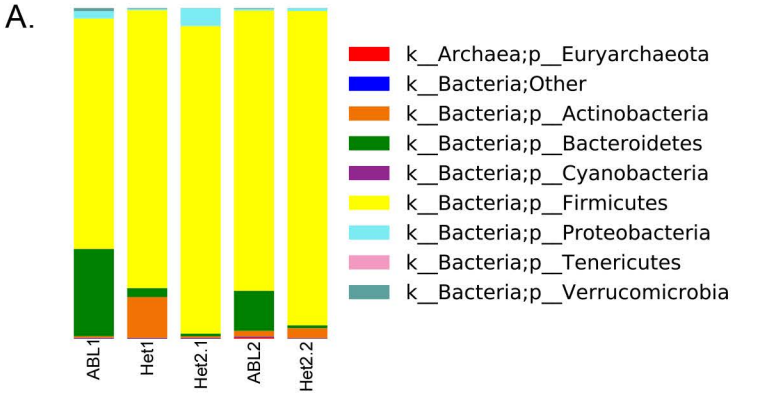

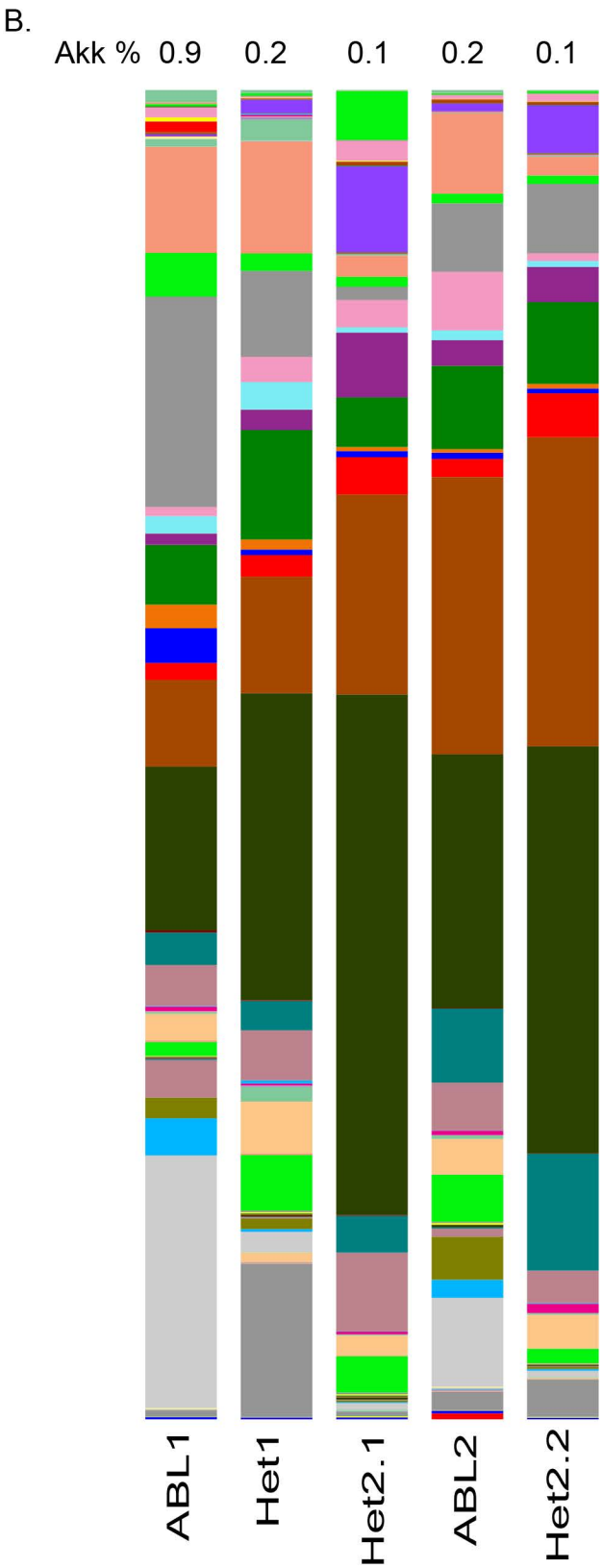

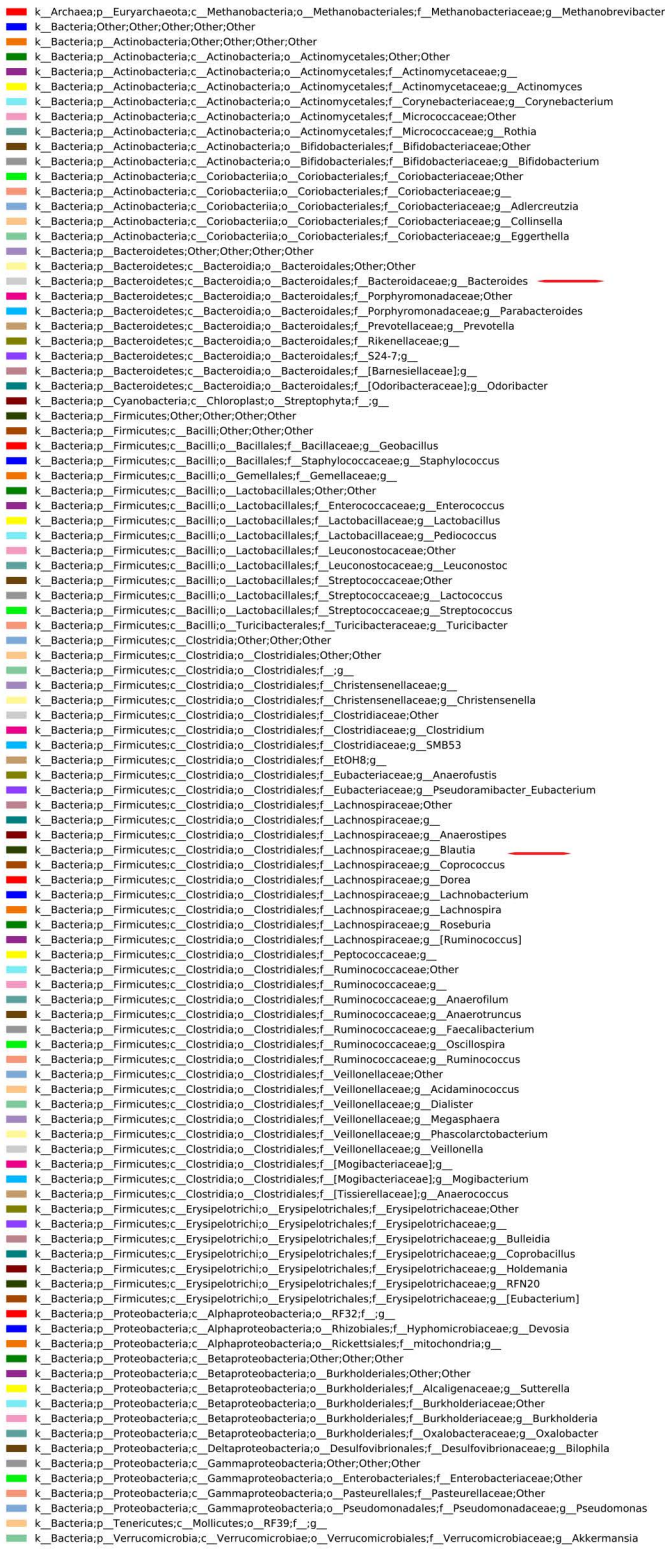

Supplemental Figure S11

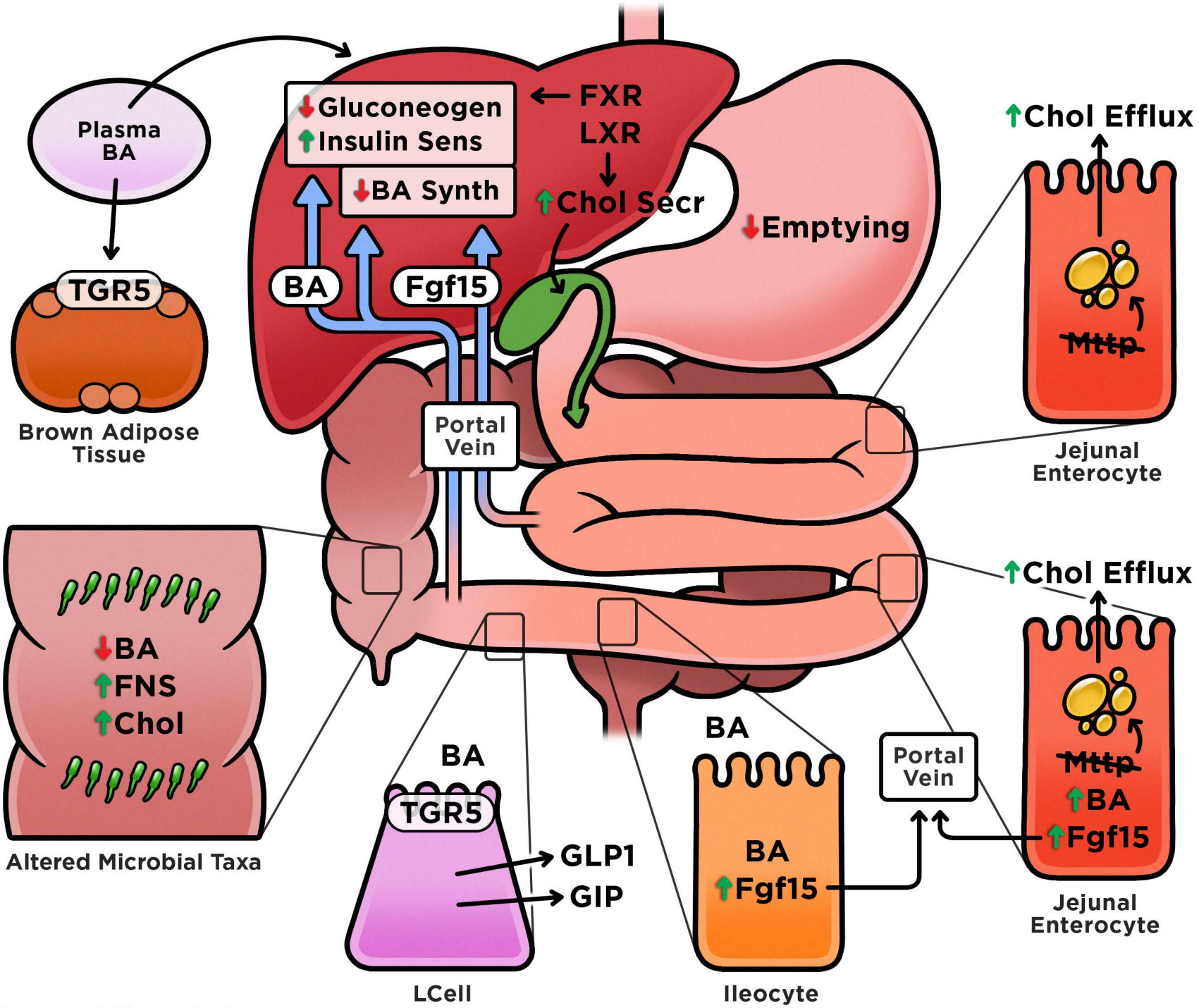

Supplemental Figure S12